Use of rapid small-scale column tests for simultaneous prediction of phosphorus and nitrogen retention in large-scale filters

Published as: Ezzati, G., Healy, M.G., Christianson, L., Daly, K., Fenton, O., Feyereisen, G., Thornton, S., Callery, O. 2020. Use of rapid small-scale column tests for simultaneous prediction of phosphorus and nitrogen retention in large-scale filters. Journal of Water Process Engineering 37: 101473. https://doi.org/10.1016/j.jwpe.2020.101473

Use of rapid small-scale column tests for simultaneous prediction of phosphorus and nitrogen retention in large-scale filters

G. Ezzati[1, 2], M.G. Healy[2], L. Christianson[3], K. Daly[1], O. Fenton[1*], G. Feyereisen[4], S. Thornton[5], O. Callery[6]

[1] Teagasc, Environmental Research Centre, Johnstown Castle, Co. Wexford, Ireland

[2] Civil Engineering and Ryan Institute, College of Science and Engineering, National University of Ireland, Galway, Galway, Ireland

[3] Department of Crop Sciences, University of Illinois at Urbana-Champaign, Urbana, IL, USA

[4] USDA-Agricultural Research Service (ARS), St. Paul, MN, USA

[5] Groundwater Protection and Restoration Group, Kroto Research Institute, University of Sheffield, Sheffield, United Kingdom

[6] Earth and Ocean Sciences and Ryan Institute, College of Science and Engineering, National University of Ireland, Galway, Galway, Ireland

*Corresponding author: owen.fenton@teagasc.ie

Abstract

Rapid small-scale column tests (RSSCTs) have been previously used to predict the effluent concentration of a single nutrient in large filters with good accuracy. However, in drainage waters originating from heavy textured soils, where there is a need for in-ditch filters to retain

both dissolved reactive phosphorus (DRP) and ammonium (NH_4) simultaneously, the suitability of a RSSCT approach to model both parameters must be proved. In this study, a decision support tool was used to identify appropriate media that may be placed in filters for the removal of DRP and NH_4. The selected media for this study were sand and zeolite. Both media were placed in acrylic tubes each with an internal diameter of 0.01 m and with lengths ranging from 0.1 to 0.4 m, and their performance for simultaneous removal of DRP and NH_4 (1 mg DRP and NH_4-N L^{-1}) from water was evaluated. The data generated from the RSSCTs were used to model DRP and NH_4 removals in 0.4 m-long laboratory columns of internal diameter 0.1m, which had the same media configuration as the small columns and were operated using the same influent concentrations. The developed model successfully predicted the effluent concentration of both the DRP and NH_4-N from the large columns. This indicates using RSSCTs to model the performance of filters will produce substantial savings in operational, financial and labour costs, without affecting the accuracy of model predictions.

Keywords: adsorption, phosphorus, ammonium, agriculture, drainage, water

1. Introduction

Intensification of agriculture through crop growth strategies and increased animal stocking rates has been enacted in many countries of the European Union (EU) (Van Zanten et al., 2016). This may result in unabated diffuse and point-source nutrient (nitrogen (N) and phosphorus (P)) losses to water bodies, causing multiple effects on environmental systems while traveling along biogeochemical pathways and continua from soil to water bodies (Galloway et al., 2003; Sharpley et al., 2011). As surface and subsurface storage components of these mixed nutrients are large, critical and incidental losses which are deleterious for the aquatic system, will occur

(Schulte et al., 2014; Ascott et al., 2018). Therefore, alongside existing best management practices to mitigate surface and groundwater nutrient losses, there is a need for a number of additional measures that can intercept and mitigate nutrients before they leave the farm system. Engineered remediation technologies, often referred to as engineered structures, are amongst these measures and have moved beyond proof of concept in recent years (Christianson and Schipper, 2016). These are placed at nutrient pollution delivery points in hydrologically active areas (Penn et al., 2017), where the soil natural attenuation capacity does not exist or has already been exhausted due to accumulation of nutrients (Ezzati et al., 2020). These structures include installation of structures filled with P sorbing materials (Penn et al., 2014a; Sanford and Larson, 2016) to intercept surface runoff, in-ditch control structures designed to remove both P and N in drainage waters (Fenton et al., 2016), and denitrifying bioreactors connected to tile systems that are filled with carbon-based media that convert nitrate (NO_3) to di-nitrogen gas (Christianson et al., 2013; Healy et al., 2014; Fenton et al., 2016). Efforts are now being made to make the use of engineered structures as a sustainable pollution remediation technique that takes local, environmental and financial conditions of the user into consideration.

Ezzati et al. (2019) developed a decision support tool (DST) to assist users in the selection of locally sourced media for use in mitigating pollution associated with excess nutrients in drainage waters which incorporates several factors important in choosing filter media such as lifespan, hydraulic conductivity, the potential for pollution swapping, attenuation of non-target contaminants (e.g. pesticides, organic carbon, etc.), local availability, and costs associated with transporting media to site. Within this DST, several water contamination scenarios were identified, such as NO_3 only, dissolved reactive phosphorus (DRP) only, or a mixed discharge of ammonium (NH_4) and DRP.

On heavy textured soils, where land drainage has been installed to extend the grazing season, there is a large body of evidence (e.g. Clagnan et al., 2019) that identifies NH_4 (not NO_3) and DRP as the main nutrients of concern in both shallow and groundwater drainage systems. The aim of the current study is to design and quantify the effectiveness of small filters containing appropriate media capable of retaining both NH_4 and DRP.

Prior to deployment of filters in field situations, it is advisable to characterise the adsorption capacity of the media using batch experiments. These tests are quick, cheap, and easy-to-perform (Crini and Badot, 2008), but fail to replicate in-field conditions, in which there may be additional variables, such as fluctuating water temperatures, flow dynamics and pollutant loads. Consequently, they often fail to accurately estimate lifespan or effectiveness of the media (Pratt and Shilton, 2009). As the accurate estimation of long-term performance of a medium is only possible under continuous flow conditions in the field (Pratt et al., 2012), the closest simulation to in-field conditions is to allow nutrient-rich water to flow through large-scale adsorption columns which are frequently operated in the laboratory (Nwabanne and Igbokwe, 2012; Monrabal-Martinez et al., 2017). However, these tests are costly and may take a long period to reach steady-state conditions (Penn et al., 2014b).

Rapid small-scale column tests (RSSCTs), which use only a minimum quantity of medium and contaminant solution, have been developed to reproduce the results of large-scale column studies (Poddar, 2013). Callery et al. (2016) used RSSCTs to predict the long-term P retention performance of large-scale, single medium adsorption filters. Callery and Healy (2017) developed the model further to predict medium saturation, as well as filter-pore and effluent concentration data. This RSSCT and modeling approach has never been attempted to examine a mixed contaminant scenario such as that found in heavy textured soils i.e. the simultaneous

106 treatment of DRP and NH_4. Such a scenario would necessitate the presence of more than one
107 medium in a filter that would retain both nutrients of environmental concern in drainage waters.
108
109 Therefore, the objective of the current study is to examine the efficacy of the RSSCT modeling
110 approach in predicting DRP and NH_4 effluent concentration that simultaneously pass through
111 large-scale columns filled with two media. If this methodology proves successful, this approach
112 may provide an accurate and quick method of predicting the performance of filter media that
113 may negate the need for long-term and expensive large-scale column studies.
114
115 **2. Materials and Methods**
116
117 *2.1 Media selection using batch experiments and falling head tests*
118 The DST, developed by Ezzati et al. (2019), was used to generate a list of media capable of
119 mitigating DRP and NH_4 in drainage water (Table 1 - Stage 1). Batch and adsorption isotherm
120 experiments were conducted to identify media with the highest adsorption capacities for DRP
121 and NH_4 (Table 1 - Stage 2). The batch experiments were conducted as follows: 2 g of locally
122 sourced media, identified in Stage 1, were placed in 50 ml-capacity glass containers. Each
123 medium was overlain with 35 ml of distilled water, which was amended with both KH_2PO_4
124 and NH_4Cl to produce mixed DRP and NH_4-N solutions with concentrations ranging from 1
125 mg L^{-1} to 40 mg L^{-1}. The containers were then sealed and placed in an end-over end shaker for
126 24 h. Following this, the samples were allowed to settle for 1 h and then centrifuged at 3500
127 rpm for 10 min, before the supernatant was withdrawn and filtered using 0.45-μm filters. All
128 water samples were analysed for DRP and NH_4-N within 24 h using a Thermo Konelab 20
129 analyser (Technical Lab Services, Ontario, Canada). A multipoint Langmuir isotherm
130 (McBride, 2000) was used to estimate the adsorption capacity of each medium. The specific

adsorption (q_e) (the mass of nutrient adsorbed per unit mass of amendment at equilibrium) (g kg^{-1}) was calculated from the following equation (McBride, 2000):

$$q_e = (C_0 - C_e) * \frac{V}{M} \quad \text{[Eqn. 1]}$$

where C_e is the concentration of nutrient (DRP or NH_4-N) in solution at equilibrium (mg L^{-1}), C_0 is initial concentration, V is the volume of solution (L), and M is the weight of adsorbent medium (g). q_{max}, an estimate of the maximum monolayer adsorption capacity of the media, was calculated by plotting q_e/C_e against C_e and using the slope and intercept from the following equation (McBride, 2000):

$$\frac{C_e}{q_e} = \frac{1}{b} * q_{max} + C_e/q_{max} \quad \text{[Eqn. 2]}$$

where b is the coefficient associated with adsorption energy (L mg^{-1}) to form a complete monolayer on the surface.

The average retention efficiency S (%) (Penn et al., 2010) was calculated as follows:

$$S = \frac{C_e - C_o}{C_o} * 100 \quad \text{[Eqn. 3]}$$

where C_e and C_0 are as defined above.

A constant head method (ASTM D2434; ASTM, 2000) was used to measure the saturated hydraulic conductivity (K_{sat}, m d^{-1}) of the media selected in Stage 2 (Table 1 – Stage 3). This

parameter helps in avoiding filter clogging and is considered to be one of the factors that ensures effective operation of filters (Segismundo et al., 2017). The elemental composition of selected media was analysed with a Rigaku NEX CG energy dispersive X-ray fluorescence bench-top spectrometer (EDXRF; Rigaku, Austin, USA).

2.2 Preparation of filter columns

In this experiment, two sets of filter columns were constructed: small columns, with lengths ranging from 0.1 to 0.4 m (internal diameter 0.01 m), and large columns with lengths of 0.4 m (internal diameter 0.1 m) (Figure 1 and Figure S1 in the Supplementary Material). For both scales the selected media for DRP and NH_4 retention was sand and zeolite, respectively. The packing density for sand and zeolite was 1.8 g cm^{-3} and 0.92 g cm^{-3}, respectively.

Each large column was instrumented with an inlet pipe at the base and an outlet pipe, which was positioned 0.38 m from the base (after the second media). The media overlay a fine metal mesh, positioned 0.01 m from the base to prevent clogging and to allow for uniform water distribution. The columns were positioned vertically and fixed on a steel frame, with flow entering the bottom of the columns. For the large columns, two media configurations were used to investigate possible differences in nutrient breakthrough. Such an aspect is important in real world filters, where the first medium acts as a bulk removal medium with a large capacity for the contaminant, and the second medium captures the low concentration of the remaining contaminant (e.g. DRP) before discharge. The media configurations were as follows: sand over zeolite or zeolite over sand (each at n=3) and each layer was 0.19 m deep, giving a total depth of filter media of 0.38 m

For the small columns, polycarbonate tubes with an internal diameter of 0.01 m and lengths of 0.1, 0.2, 0.3, and 0.4 m were used (Figure 1 (b)). Plastic syringes were connected to either end of the columns, into which acid-washed glass wool (2 g) was placed to retain the media and avoid microbial growth. The columns were positioned vertically and fixed in retort stands, with flow entering the bottom of the columns. As media configuration change made no difference to retention (Section 3.2), a single configuration was chosen i.e. zeolite over sand. To achieve a similar packing density to the large columns for each column length, a mass of 12.4, 24.9, 37.4 and 49.7 g of sand and 6.3, 12.7, 19.1 and 25.5 g of zeolite were used for the 0.1, 0.2, 0.3 and 0.4 m columns, respectively.

2.3 Operation of the filter units

Prior to the start of the experiment, potable water was pumped through the small and large columns to remove background concentrations of DRP and NH_4. When the outlet concentrations were < 0.01 mg DRP L^{-1} and < 0.01 mg NH_4-N L^{-1}, the experiment commenced. KH_2PO_4 and NH_4Cl were used to produce mixed influent water for the large and small columns with concentrations of 1 mg DRP L^{-1} and 1 mg NH_4-N L^{-1}. As the objective of the study was to examine the efficacy of the RSSCT modeling approach in predicting DRP and NH_4 effluent concentration, effects such as competitive adsorption between multiple contaminants were not examined.

Peristaltic pumps were used to pump the influent water to the large columns at a hydraulic loading rate (HLR) of 156 cm d^{-1}, which is similar to the HLR applied in onsite wastewater filtration systems (Hermann et al., 2013). The large columns were operated for 42 d, with the pumps operational for 5 h per day.

For the small columns, influent water (with a concentration of 1 mg DRP L^{-1} and 1 mg NH_4-N L^{-1}) was pumped into the base of the columns at a HLR 52.8 cm d^{-1} for 6 h per day. The HLR was chosen so as the median empty bed contact time (EBCT) of the small columns was similar to the large columns. The duration of the small column experiment was 11 d, which was the length of time over which both DRP and NH_4-N removals dropped below 100% to provide enough data for model generation.

2.4 Data collection and analysis

For both column scales, the influent (daily) and effluent (different time points) were sampled in 50 mL tubes and filtered immediately through 0.45 μm filters and analysed for DRP and NH_4-N within 24 h using a Thermo Konelab 20 analyser (Technical Lab Services, Ontario, Canada). During the first 4 days of operation of the large columns, the effluent was sampled after every bed volume. After reaching steady-state conditions (defined as the point at which the effluent concentration began to stabilise), sampling was increased to every 5 bed volumes for another 2 days, and later on increased to every 10 bed volumes. For the small columns, sampling was conducted every two hours. On each sampling occasion, two samples were taken from each column: a sample (5 ml) was taken directly from the effluent (marking the end of the 2-h period and compared with the influent daily concentration) and a sub-sample (50 ml) was taken from the total filtered volume in that 2-h composite period.

In order to model the effluent concentrations of nutrients leaving the large and small columns, the adsorption model of Callery and Healy (2017) was used, assuming that pseudo-second order kinetics was occurring for both nutrients (Jiang et al., 2013; Olgun et al., 2013; Sieczka and Koda, 2016; Riahi et al., 2017; Wasielewski et al., 2018):

$$C_t = C_0 - [((A\, V_B^{(\frac{1}{B})} M))/VB] * [t/(t+K)] \quad \text{[Eqn. 4]}$$

where C_t is the filter effluent concentration (mg L^{-1}), C_o is the influent concentration (mg L^{-1}); A, B and K are coefficients representing a constant of proportionality (mg g^{-1}), a constant of system heterogeneity (i.e. existence of multiple types of adsorption sites in the medium) (no units), and a time constant (min), respectively; V_B is the empty bed volumes (the volume of the filter without media) of filtered solution (no units), M is the mass of adsorbent (g), V is the volume of filtered solution (L), and t the empty bed contact time (min) (the average retention time in an empty filter). A coded MS Excel™ file is given in the Supplementary Material.

The coefficients (A, B, and K), determined from the small column study, were fitted using the Levenberg-Marquant algorithm via Solver in Excel to give the least error squared (ERRSQ) of difference between the predicted and the actual effluent concentrations. They were then applied to predict the effluent concentration of the large columns.

As the concentration of NH_4 effluent in the 0.2 to 0.4 m columns was zero during the early bed volumes of the experiment (i.e. 100% retention was achieved initially), data for the modelling process was taken after 12 bed volumes for all column sizes. From this period onwards, the % retention in the columns dropped below 100%.

2.5 Statistics

To assess if there were any differences in % of nutrient retention capacity based on media configuration in the large columns i.e. sand over zeolite or zeolite over sand, a z-test was

conducted. A p value of < 0.05 rejected the null hypotheses i.e. no difference in terms of retention based on the configuration.

3. Results and discussion

3.1 Selection of media

The final selected media for the small and large column experiments were coarse sand (particle size 1-2 mm) sourced from the south west of Ireland with a high iron (Fe) content and natural Turkish (Yildizeli) zeolite (particle size 1-3 mm). Batch experiment results indicated that both the sand and zeolite had good DRP and NH_4 removals, and had good K_{sat} values for the column experiments (Table 2).

The sand had a q_{max} of 8.34 g DRP kg^{-1} with a binding energy, k, of 2.87 L mg^{-1} (Table 2) This q_{max} was higher than other sands commonly used in filter systems (e.g. Danish sands, which have 0.02 to 0.13 g DRP kg^{-1}; Fenton et al., 2008). Zeolite, which is an aluminosilicate mineral, also had good DRP retention, similar to the results of other studies (Lin et al., 2014; Gérard, 2016; Ibrahim et al., 2015).

Zeolite, used in the current study to target NH_4 removal, had an aluminium (Al) content of 12.8% (Table 2), which is within the range of commonly used filter P materials (i.e. 1.3 to over 40%) (Cucarella and Renman, 2009). According to Penn et al. (2017), high Fe and Al content of a P-sorption material indicates ligand exchange (ion binding to a metal) as the main mechanism for DRP retention rather than precipitation, which would occur in high calcium content materials. Zeolite had a q_{max} of 39.5 g NH_4-N kg^{-1} with a binding energy of 9.8 L mg^{-1} (Table 2). The NH_4-N retention mechanism was either molecular adsorption or ion exchange

(Zhang et al., 2011). Various ranges of q_{max} for zeolite are found in the literature due to variations in country of origin and chemical element (Wasielewski et al., 2018) e.g. 15.3-25 g NH_4-N kg^{-1} (Langwald, 2008; Zhang et al., 2010; Kotoulas et al., 2019), 31.9 g NH_4-N kg^{-1} (Ham et al., 2018), and 40.3 g NH_4-N kg^{-1} (Ibrahim et al., 2015). These have resulted in 84% to complete NH_4-N removal (99%), depending on operational conditions such as influent concentration, temperature, pH, and adsorbent dosage.

3.2 Retention of DRP and NH_4-N in the columns

For the large columns, the DRP retention was initially high at >95% for the first two empty bed volumes, V_B, of filtered solution, and decreased gradually to 13% after >100 pore volumes (43 V_B) (Figure 2). One hundred percent NH_4-N retention was achieved for the first 25 pore volumes, but decreased to 80% after 120 pore volumes (52 V_B) (Figure 3). Similar trends in NH_4-N retention using zeolite were also documented by other studies (Alshameri et al., 2014; Huang et al., 2015; Kotoulas et al., 2019). Clinoptilolite zeolite is known to be a very good ion-exchanger (Wasielewski et al., 2018), and a high adsorption rate has been associated with diffusion of NH_4-N ions (Huang et al., 2010) through macropores and mesopores to the surface of zeolite (Shaban et al., 2017).

The configuration of the media did not affect DRP or NH_4 retentions ($p > 0.05$). The use of dual media, placed side by side in a filter with each designed to adsorb either P or N from different wastewater types has been previously investigated (e.g. Goodwin et al., 2015) and, similar to the current study, other studies have found that configuration of the media (N adsorbing media before P adsorbing media, or vice versa) does not affect P or N removal (Christiansen et al., 2017).

302 The small columns were P-saturated after 1 L of filtered volume (V_B=50 for the 0.3 m
303 column), whereas the NH_4 saturation of the columns took substantially longer to occur; the
304 0.1 m column was 80% saturated after approximately 10 L filter volumes (V_B=1550) and
305 duration of complete removal was related to the length of the column. Unlike many batch
306 adsorption experiments and large-scale column tests examining the NH_4 removal efficiency
307 of zeolite, RSSCTs operated under continuous loading of a few hours per day has never been
308 investigated. However, the results here are in agreement with other studies, which showed a
309 positive relationship between removal efficiency, mass of adsorbent and contact time
310 (Kotoulas et al., 2019).
311
312 *3.3 Predicting DRP effluent concentration in large columns using scale column data*
313 Regardless of media configuration, the model developed using the small column data (Table
314 3, ERRSQ=5.56) was able to predict the trend of DRP effluent in the large columns. Figure 2
315 superimposes the modelled data from the small columns onto the measured data from the
316 large columns and Figure 4 presents the observed versus modelled data using coefficients
317 from small column tests for each individual column and configuration.
318
319 The constant of heterogeneity, B, was a dominant coefficient in predicting effluent
320 concentrations. This is indicative of potentially multiple adsorption mechanisms responsible
321 for nutrient removal which can be explained by the fact that the model is predicting combined
322 removal efficiency of two media with different elemental compositions (Table 2), which are
323 packed into one filter column. According to Callery and Healy (2017), the curve produced by
324 Eqn. 4, which is based on second-order kinetics, can indicate the importance of intraparticle
325 diffusion (Ko et al., 2000) for model prediction within small columns at different lengths.
326 This is shown in Figure 2, where the tailing of the breakthrough curve has likely been caused

by intra-particle diffusion (Doekar and Mandavgane, 2015). This may become significant as the surface of the medium/media become saturated or as EBCT increases (Callery and Healy, 2017).

3.4 Predicting NH_4-N effluent concentration from large columns using small columns

Complete NH_4-N removal was observed during the initial operational period of the large and small columns, which is consistent with other studies (Balci and Dince, 2002; Sharifnia et al., 2016; Mazloomi and Jalali, 2016; Kotoulas et al., 2019). Consequently, the small columns were operated for a longer period of time (11 d in total) to generate enough data for the successful prediction of NH_4-N effluent concentrations leaving the large columns.

Eqn. 4 predicted the behaviour of the filters in retaining NH_4-N (Figure 3) and Figure 5 presents observed versus modelled data using coefficients from small column tests for each individual column. The constant of heterogeneity in NH_4-N adsorption, B, was less than DRP (Table 4), which indicates that zeolite, not sand, was the only medium in the columns capable of NH_4-N retention as also observed in the batch experiment. However, the high K values indicate that the adsorption rate did not follow a linear regression with filter depth, as initially proposed by filter bed depth service time (BDST) (Hutchins, 1973) which has been used by many adsorption studies. The BDST model assumes that intraparticle diffusion is negligible (Ayoob and Gupta, 2007), which becomes an important factor as a medium's surface becomes more saturated (Doekar and Mandavgane, 2015; Callery and Healy, 2017). The proposed model in this study is therefore describing a real-world adsorption system in which several factors control the adsorption (Crini and Badot, 2010), meaning that larger amounts of media and increased contact time may not produce directly proportionally higher adsorption. A similar lack of proportionality between the length of columns (amount of adsorbent) and increase in NH_4-N

retention has been reported by Sarioğlu (2004). Although the experiments were carefully designed to provide similar environmental conditions for all columns, there was a small difference between data generated from various large-scale columns. In order to avoid any bias, average effluent data were used to generate model parameters.

3.6 Implications of study for drainage filters

To date, large-scale columns have been mainly used to estimate nutrient saturation and longevity of media to replicate operational conditions (Peyne et al., 2014; Lopez-Ponnada et al., 2017; Monrabal-Martinez et al., 2017). However, moving from large-scale columns to RSSCTs would gain financial and labour advantages, whilst not sacrificing the accuracy of model outcomes. This may include considerable savings on: time required for constructing and operating the columns, labour hours and number of staff required, space required to house the structure and experimental set up, number/capacity of containers, amount of influent (chemical and distilled water), procurement of adsorbent(s) (media) and sampling equipment e.g. tubes, syringes, filter pours; number of pumps, cost of laboratory analysis of water samples; and overhead costs, including electricity and light.

The results of this study validated the model, showing that it could upscale RSSCTs accurately to describe the pattern of large-scale column performance. However, it is important to design the experiment carefully so as the media becomes partially saturated over the duration of the experiment. In the current study, the modelling parameters of Eqn. 4 predicted the NH_4-N effluent concentration in the large columns only after the retention of NH_4-N in the small columns dropped to below 100%.

Figure 6 presents a flowchart which shows steps towards the implementation of an efficient field-scale engineered structure filled with adsorptive media, to treat DRP and NH_4-N in drainage water. In general, a successful implementation includes characterisation of nutrient losses in the farm, correct choice of medium/media with a high nutrient retention capacity (and which does not contribute to pollution swapping; Ezzati et al., 2019), characterisation of the retention capacity, and therefore lifetime, of the selected media, and the identification of an optimal location for installation of structure (Ezzati et al., 2020). This would ultimately provide a sustainable and cost-effective mitigation for the removal of mixed contaminants in agricultural ditches.

4. Conclusions

In this study, rapid small scale column tests were used to predict effluent DRP and NH_4-N concentrations from much larger columns with good accuracy. As large-scale laboratory filter column tests are time consuming and expensive, but are considered to replicate in-field conditions well, the methodology used in this study will save operational, financial and labour costs, whilst providing good model predictions of DRP and NH_4-N. Future work should consider modelling biological N removal (e.g. nitrate) in filters containing C-rich media (e.g. woodchip), where adsorption is not the dominant removal mechanism. In addition, research should focus on potential uses for saturated filter media.

Acknowledgements

This project has received funding from the European Union's Horizon 2020 research and innovation programme under the Marie Skłodowska-Curie grant agreement No 675120.

401 **References**

402

403 Alshameri, A., Ibrahim, A., Assabri, A.M., Lei, X., Wang, H., Yan, C., 2014. The
404 investigation into the ammonium removal performance of Yemeni natural zeolite:
405 Modification, ion exchange mechanism, and thermodynamics. Powder Technology, 258, 20-
406 31.

407 Ascott, M., Gooddy, D., Lapworth, D., Davidson, P., Bowes, M.J., Jarvie, H., Surridge, B.,
408 2018. Phosphorus fluxes to the environment from mains water leakage: Seasonality and future
409 scenarios. Science of the Total Environment, 636, 1321-1332.

410 ASTM D2434, 2006. Standard Test Method for Permeability of Granular Soils
411 (Constant Head). American Society for Testing and Materials, PA.

412 Ayoob, S., Gupta, A.K., 2007. Sorptive response profile of an adsorbent in the
413 defluoridation of drinking water. Chemical Engineering, 133, 273-281.

414 Balci, S., Dince, Y., 2002. Ammonium ion adsorption with sepiolite: use of transient
415 uptake method. Chemical Engineering Process, 41, 79-85.

416 Callery, O., Healy, M.G., Rognard, F., Barthelemy, L., Brennan, r.B., 2016. Evaluating
417 the long-term performance of low cost adsorbents using small-scale adsorption column
418 experiments. Water Research. 101, 429-440.

419 Callery, O., Healy, M.G., 2017. Predicting the propagation of concentration and
420 saturation fronts in fixed-bed filters. Water Research. 123, 556- 568.

421 Clagnan, E., Thornton, S.F., Rolfe, S.A., Wells, N.S., Knöller, K., Murphy, J., Tuohy, P.,
422 Daly, K., Healy, M.G., Ezzati, G., von Chamier, J., Fenton, O., 2019. An integrated
423 assessment of nitrogen source, transformation and fate within an intensive dairy system to
424 inform management change. PLOS ONE, 14.

425 Christianson, L.E, Schipper, L., 2016. Moving denitrifying bioreactors beyond proof of
426 concept: Introduction to the special section. Environmental Quality, 45, 757-761.

427 Christianson, L.E, Tyndall, J., Helmers, M., 2013. Financial comparison of seven nitrate
428 reduction strategies for Midwestern agricultural drainage. Water Resources and Economics,
429 2, 30-56.

Christianson, L.E., Lepine, C., Sibrell, P.L., Penn, C., Summerfelt, S.T., 2017. Denitrifying woodchip bioreactor and phosphorus filter pairing to minimize pollution swapping. Water Research, 121, 129-139.

Crini, G., Badot, P.M., 2008. Application of chitosan, a natural aminopolysaccharide, for dye removal from aqueous solutions by adsorption processes using batch studies: a review of recent literature. Progress in Polymer Science, 33, 399-447.

Cucarella, V., Renman, G., 2009. Phosphorus sorption capacity of filter materials used for on-site wastewater treatment determined in batch experiments–A comparative study. Environmental Quality, 38, 381-92.

Doekar, S.K., Mandavgane, S.A., 2015. Estimation of packed-bed parameters and prediction of breakthrough curves for adsorptive removal of 2,4-dichlorophenoxyacetic acid using rice husk ash. Environmental Chemical Engineering, 3, 1827-1836.

Ezzati, G., Healy, M., Christinson, L., Feyereisen, G., Daly, K., Thornton, S., 2019. Developing and validating an adaptable decision support tool (FarMit) for selection of locally sourced media for dual mitigation of nutrients in drainage water from intensively farmed landscapes. Ecological Engineering, 2.

Ezzati, G., Fenton, O., Healy, M.G., Christianson, L., Feyereisen, G.W., Thornton, S., Chen, Q., Fan, B., Ding, J., Daly, K., 2020. Impact of P inputs on source-sink P dynamics of sediment along an agricultural ditch network. Environmental Management, 257, 109988.

Fenton, O., Healy, M.G., Schulte, R.P.O., 2008. A review of remediation and control systems for the treatment of agricultural waste water in Ireland to satisfy the requirements of the water framework directive. Biology and Environment: Proceeding of the Roal Irish Academy, 108B, No. 2, 69-79.

Fenton, O., Healy, M.G., Brennan, F.P., Thornton, S.F., Lanigan, G.J., Ibrahim, T.G., 2016. Holistic Evaluation of Field-Scale Denitrifying Bioreactors as a Basis to Improve Environmental Sustainability. Environmental Quality, 45, 788-795.

Galloway, J. N., Aber, J. D., Erisman, J. W. et al., 2003. The nitrogen cascade. Bioscience, 53, 341–356.

Gérard, F., 2016. Clay minerals, iron/aluminum oxides, and their contribution to phosphate sorption in soils—A myth revisited. Geoderma, 262, 213–226.

460 Goodwin, G.E., Bhattarai, R., Cooke, R., 2015. Synergism in nitrate and orthophosphate
461 removal in subsurface bioreactors. Ecological Engineering, 84, 559-568.

462 Ham, K., Kim, B.S., Choi, K-Y., 2018. Enhanced ammonium removal efficiency by ion
463 exchange process of synthetic zeolite after Na^+ and hear pretreatment. Water Science &
464 Technology, 78, 1417- 1425.

465 Healy, M.G., Barrett, M., Lanigan, G., Serrenho, A., Ibrahim, T.G., Thornton, S.F., Rolfe,
466 S.A., Huang, W.E., Fenton, O., 2014. 'Optimizing nitrate removal and evaluating pollution
467 swapping trade-offs from laboratory denitrification bioreactors'. Ecological Engineering, 74,
468 290-301

469 Herrmann, I., Jourak, A., Hedström, A., Lundström, T.S., Vilander, M., 2013. The Effect
470 of Hydraulic Loading Rate and Influent Source on the Binding Capacity of Phosphorus Filters.
471 PLOS ONE, 8.

472 Huang, H., Xiao, X., Yan, B., Yang, L., 2010. Ammonium removal from aqueous solutions
473 by using natural Chinese (Chende) zeolite as adsorbent, J. Hazard Mater., 175, 247-252.

474 Huang, H.; Yang, L.; Xue, Q.; Liu, J.; Hou, L.; Ding, L., 2015. Removal of ammonium
475 from swine wastewater by zeolite combined with chlorination for regeneration.
476 Environmental Management. 160, 333–341.

477 Hutchins, R., 1973. New method simplifies design of activated carbon systems, water bed
478 depth service time analysis. Chemical Engineering, 81, 133-138.

479 Ibrahim, T.G., Goutelle, A., Healy, M.G., Brennan, R., Tuohy, P., Humphreys, J., Lanigan,
480 G., Brechignac, J., Fenton, O., 2015. Mixed agricultural pollutant mitigation using
481 woodchip/pea gravel and woodchip/zeolite permeable reactive interceptors. Water Air & Soil
482 Pollution. 226.

483 Jiang, X., Bol, R., Willbold, S., Vereecken, H., Klumpp, E., 2015. Speciation and
484 distribution of P associated with Fe and Al oxides in aggregate-sized fraction of an arable soil,
485 Biogeosciences, 12, 6443–6452.

486 Ko, D.C.K., Porter, J.F., McKay, G., 2000. Optimised correlations for the fixed-bed
487 adsorption of metal ions on bone char. Chemical Engineering Science, 55, 5819-5829.

488 Kotoulas, A., Agathou, D., Triantaphyllidou, I.E., Tatoulis, T.I., Akratos, C.S.,
489 Tekerlekopoulou, A.G., Vayenas, D.V., 2019. Article Zeolite as a Potential Medium for
490 Ammonium Recovery and Second Cheese Whey Treatment, Water, 11.

KuČiĆ, D., MarkiĆ, M., BriŠKi, F., 2012. Ammonium Adsorption on Natural Zeolite (Clinoptilolite): Adsorption Isotherms and Kinetics Modelling. The Holistic Approach to Environment, 2, 145-158.

Langwaldt, J., 2008. Ammonium removal from water by eight natural zeolites: A comparative study. Separation Science and Technology, 43, 2166- 2182.

Lin, L., Wan, C., Lee, D-J., Lei, Z., Liu, X., 2014. Ammonium assists orthophosphate removal from high-strength wastewaters by natural zeolite. Separation and purification technology, 133, 351-356.

Lopez-Ponnada, E.V., Lynn, T.J., Peterson, M., Ergas, S.J., Mihelcic, J.R., 2017. Application of denitrifying wood chip bioreactors for management of residential non-poin sources of nitrogen. Biological Engineering, 11.

Mazloomi, F., Jalali, M., 2015. Ammonium removal from aqueous solutions by natural Iranian zeolite in the presence of organic acids, cations and anions. Environmental Chemical Engineering, 4.

McBride, M. B., 2000. Chemisorption and precipitation reactions. In: Sumner ME, editor. Handbook of soil science. Boca Raton, Fl: CRC Press; p. B-265–302.

Monrabal-Martinez, C., Ilyas, A., Muthanna, T.M., 2017. Pilot scale testing of adsorbent amended filters under high hydraulic loads for highway runoff in cold climates. Water. 9, 230.

Nwabanne, J.T., Igbokwe, P.K., 2012. Kinetic modeling of heavy metals adsorption on fixed bed column. *International Journal of Environmental Research*, **6**, 945–952.

Olgun, A., Atar, N., Wang, S., 2013. Batch and column studies of phosphate and nitrate adsorption on waste solids containing boron impurity. Chemical Engineering Journal, 222, 108-119.

Payne, E., Tracey, P., Perran, C., Tim, F., Belinda, H., Deletic, A., 2014. Biofilter design for effective nitrogen removal from stormwater- Influence of plant species, inflow hydrology and use of a saturated zone. Water science and technology: a journal of the International Association on Water Pollution, 69, 1312-1319.

Penn, C.J., Warren, J.G., Savannah, S., 2010. Maximizing ammonium nitrogen removal from solution using different zeolites. Environmental Quality, 39, 1478-1485.

520 Penn, C.J., McGrath, J., Bowen, J., Wilson, S., 2014a. Phosphorus removal structures: a
521 management option for legacy phosphorus. Soil and Water Conservation, 69, 51A-56A.

522 Penn, C.J., Bell, G., Wang, Z., McGrath, J., Wilson, S., Bowen, J., 2014b. Improving the
523 ability of steel slag to filter phosphorus from runoff. Turfgrass and Environmental Research
524 Online. 13, 1-5.

525 Penn, C., Chagas, I., Klimeski, A., & Lyngsie, G., 2017. A review of phosphorus removal
526 structures: How to assess and compare their performance. Water (Switzerland), 9, 1–22.

527 Pratt, C, Shilton AN., 2009. Suitability of adsorption isotherms for predicting the retention
528 capacity of active slag filters removing phosphorus from wastewater. Water Science
529 Technology, 59, 1673-1678.

530 Pratt, C., Parsons, A.S., Soares, A., D.Martin, B., 2012. Biologically and Chemically
531 Mediated Adsorption and Precipitation of Phosphorus from Wastewater. Current opinion in
532 biotechnology. 23, 6.

533 Poddar, M., 2013. A Review on the Use of Rapid Small Scale Column Test (RSSCT) on
534 Predicting Adsorption of Various Contaminants. IOSR Journal of Environmental Science,
535 Toxicology and Food Technology, 3, 77-85.

536 Riahi, K., Chaabane, S., Thayer, B.B., 2017. A kinetic modelling study of phosphate
537 adsorption onto Phoenix dactylifera L. date plam fibers in batch mode. Saudi Chemical
538 Society, 21, S143-S152.

539 Sanford, J.R., Larson, R.A., 2016. Evaluation of Phosphorus Filter Media for an Inline
540 Subsurface Drainage Treatment System. Journal of Environmental Quality, 45, 1919-1925.

541 Sarioğlu, M., 2004. Removal of ammonium from municipal wastewater using natural
542 Turkish (Dogantepe) zeolite. Separation and Purification Technology, 41, 1-11.

543 Schulte, R.P.O., Creamer, R.E., Donnellan, T., Farrelly, N., Fealy, R., O'Donoghue, C.,
544 O'hUallachain, D., 2014. Functional land management: a framework for managing soil-based
545 ecosystem services for the sustainable intensification of agriculture. Environmental Science
546 & Policy, 38, 45-58.

547 Shaban, M., AbuKhadra, M.R., Nasief, F.M., El-Salam, H.M.A., 2017. Removal of
548 ammonia from aqueous solutions, ground water, and wastewater using mechanically activated
549 clinoptilote and synthetic zeolite-A: Kinetic and equilibrium studies. Water Air soil Pollution,
550 228.

551 Sharifnia, S., Khadivi, M.A., Shojaeimehr, T., Shavisi, Y., 2016. Characterization,
552 isotherm and kinetic studies for ammonium ion adsorption by light expanded clay aggregate
553 (LECA). Journal of Saudi Chemical Society, 20, 342-351.

554 Sharpley, A.N., Kleinman, P.J., Flaten, D.N., Buda, A.R., 2011. Critical source area
555 management of agricultural phosphorus: experiences, challenges and opportunities. Water
556 Science & Technology, 64, 945–952.

557 Sieczka, A., Koda, E., 2016. Kinetic and equilibrium studies of sorption of ammonium in
558 the soil-water environment in agricultural areas of central Poland. Applied Sciences, 6.

559 Van Zanten, H.H.E., Meerburg, B.G., Bikker, P., Herrero, M., De Boer, I.J.M., 2016.
560 Opinion paper: The role of livestock in a sustainable diet: a land-use perspective. Animal, 10,
561 547–549.

562 Wasielewski, S., Rott, E., Minke, R., Steinmetz, H., 2018. Evaluation of different
563 clinoptilolite zeolites as adsorbent for ammonium removal from highly concentrated synthetic
564 wastewater. Water, 10.

565 Zhan, Y., Zhang, H., Lin, J., Zhang, Z., Gao, J., 2017. Role of zeolite's exchangeable
566 cations in phosphate adsorption onto zirconium-modified zeolite. Molecular liquids, 243, 624-
567 637.

568 Zhang, M., Zhang, H., Xu, D., Han, L., Niu, D., Tian B., Zhang, J., Zhang, L., Wensi, W.,
569 2011. Removal of ammonium from aqueous solutions using zeolite synthesized from fly ash
570 by a fusion method. Desalination, 271, 111-121.

571

572 **Captions for Figures**

573

574 Figure 1. Schematic diagram of large columns (a) and small columns (b).

575 Figure 2. Normalised DRP concentration (y-axis) vs. pore volume (x-axis) for both
576 configurations of the large columns. The dashed line is the model fit using coefficients from
577 small columns. Top: sand over zeolite (A, B and C). Bottom: zeolite over sand (D, E, F).

578 Figure 3. Normalised NH_4-N concentration (y-axis) vs. pore volume (x-axis) for both
579 configurations of the large columns. The dashed line is the model fit using coefficients from
580 small columns. Top: sand over zeolite (A, B and C). Bottom: zeolite over sand (D, E, F).

581 Figure 4. Observed DRP concentrations versus predicted DRP concentrations using
582 coefficients from small columns. Left: Configuration 1 (zeolite at the bottom, sand at the top)
583 (A, B, C); Right: Configuration 2 (zeolite at the top and sand at the bottom) (D, E, F).

584 Figure 5. Observed NH_4-N concentrations of large columns versus predicted NH_4-N
585 concentrations using coefficients from small columns. Left: Configuration 1 (zeolite at the
586 bottom, sand at the top) (A, B, C); Right: Configuration 2 (zeolite at the top and sand at the
587 bottom) (D, E, F).

588 Figure 6. Flow chart for the design of an in-ditch field scale engineered structure filled with
589 reactive media for a mixed discharge of NH_4-N and DRP.

590

591

592

593

594

595

Captions for Tables

Table 1. Stages of media selection for dual nutrient mitigation. At the end of each selection stage, media failing the criteria are omitted from the table.

Table 2. Batch experiment and constant head data for maximum adsorption capacity of media (q_{max}; g kg^{-1}), binding energy (k; L mg^{-1}), and selected elemental composition based on XRF analysis of sand and zeolite used in the column experiments

Table 3. Comparison of model parameters, coefficients and ERRSQ values, obtained when (a) fitting Eqn. 4 to DRP concentration data from large columns using model coefficients determined from small columns, (b) parameters at different depths of small columns.

Table 4. Comparison of model parameters, coefficients and ERRSQ values, obtained when (a) fitting Eqn. 4 to NH_4-N concentration data from large columns using model coefficients determined from small columns, (b) model parameters at different depths of small columns.

613 Table 1. Stages of media selection for dual nutrient mitigation. At the end of each selection stage, media
614 failing the criteria are omitted from the table.

Stage 1 Selection of media using a DST[1]	Stage 2 Batch & Adsorption isotherm tests	Stage 3 K_{sat} tests
Peat soil	Peat soil	
Processed Peat (Puraflo peat)	Processed Peat (Puraflo peat)	
Compost	Compost	
Woodchip	Woodchip	
Dewatered alum-sludge		
Soil (air dried at 40 ºC)		
Sand	Eight types of sands[2]	Five types of sand[2]
Turkish (Yildizeli) zeolite (particle size: 1-3 and 3-5 mm)	Turkish (Yildizeli) zeolite (particle size 1-3 and 3-5 mm)	Turkish (Yildizeli) zeolite (particle size 1-3 and 3-5 mm)
Barley straw	Barley straw (cut into 2 mm lengths)	
Maize		
Silage		

615 [1] Ezzati et al. (2019); [2] Collected from quarries in the south of Ireland
616
617
618
619
620
621
622
623
624
625
626
627

Table 2. Batch experiment and constant head data for maximum adsorption capacity of media (q_{max}; g kg^{-1}), binding energy (k; L mg^{-1}); and selected elemental composition based on XRF analysis of sand and zeolite used in the column experiments.

	q_{max} (g kg^{-1})		k (L mg^{-1})		K_{sat} (m s^{-1})	Na	Mg	Al	Si	Fe	K	Ca	Ti	S	Mn	P
	DRP	NH_4-N	DRP	NH_4-N		% of total composition[1]										
Sand	8.34	0.6	2.87		$7.41x10^{-4}$	1.3	1.0	11.8	70.9	8.6	4.0	0.1	1.2	0.4	0.2	0.1
Zeolite	6.33	39.52	2.2	9.8	$7.39x10^{-4}$	-	1.3	12.8	70.0	2.8	7.4	4.3	-	-	0.1	-

[1] Na: Sodium; Mg: Magnesium; Al: Aluminium; Si: Silicon; Fe: Iron; K: Potassium; Ca: Calcium; Ti: Titanium; S: Sulphur; Ms: Manganese; P: Phosphorus. Elements presented only for those having > 0.1% of total composition.

Table 3. Comparison of model parameters, coefficients and ERRSQ values, obtained when (a) fitting Eqn. 4 to DRP concentration data from large columns using model coefficients determined from small columns, (b) parameters at different depths of small columns.

	(a) Parameters determined using small column data	**(b) Parameters at different lengths of small columns**			
		Small column depth (m)			
Model Coefficients		0.1	0.2	0.3	0.4
A	0.03	280.56	447.05	206.32	669.24
B	2.13	18684.43	18681.93	18687.69	18682.58
K	901	897.99	846.75	972.76	877.25
ERRSQ	5.56	0.04	0.04	0.08	0.052

A: Constant of proportionality
B: Constant of system heterogeneity
K: Constant of time

Table 4. Comparison of model parameters, coefficients and ERRSQ values, obtained when (a) fitting Eqn. 4 to NH_4-N concentration data from large columns using model coefficients determined from small columns, (b) model parameters at different depths of small columns.

	(a) Parameters determined using small column data	**(b) Parameters at different lengths of small columns**			
		Small column depth (m)			
Model coefficients		0.1	0.2	0.3	0.4
A	0.057	0.051	0.048	0.11	0.11
B	1.13	1.13	1.10	1.04	1.04
K	1961.61	1961.61	1961.61	1961.63	1961.60
ERRSQ	0.13	0.11	0.12	5.23	1.75

A: Constant of proportionality
B: Constant of system heterogeneity
K: Constant of time

679 **Figure 1.**

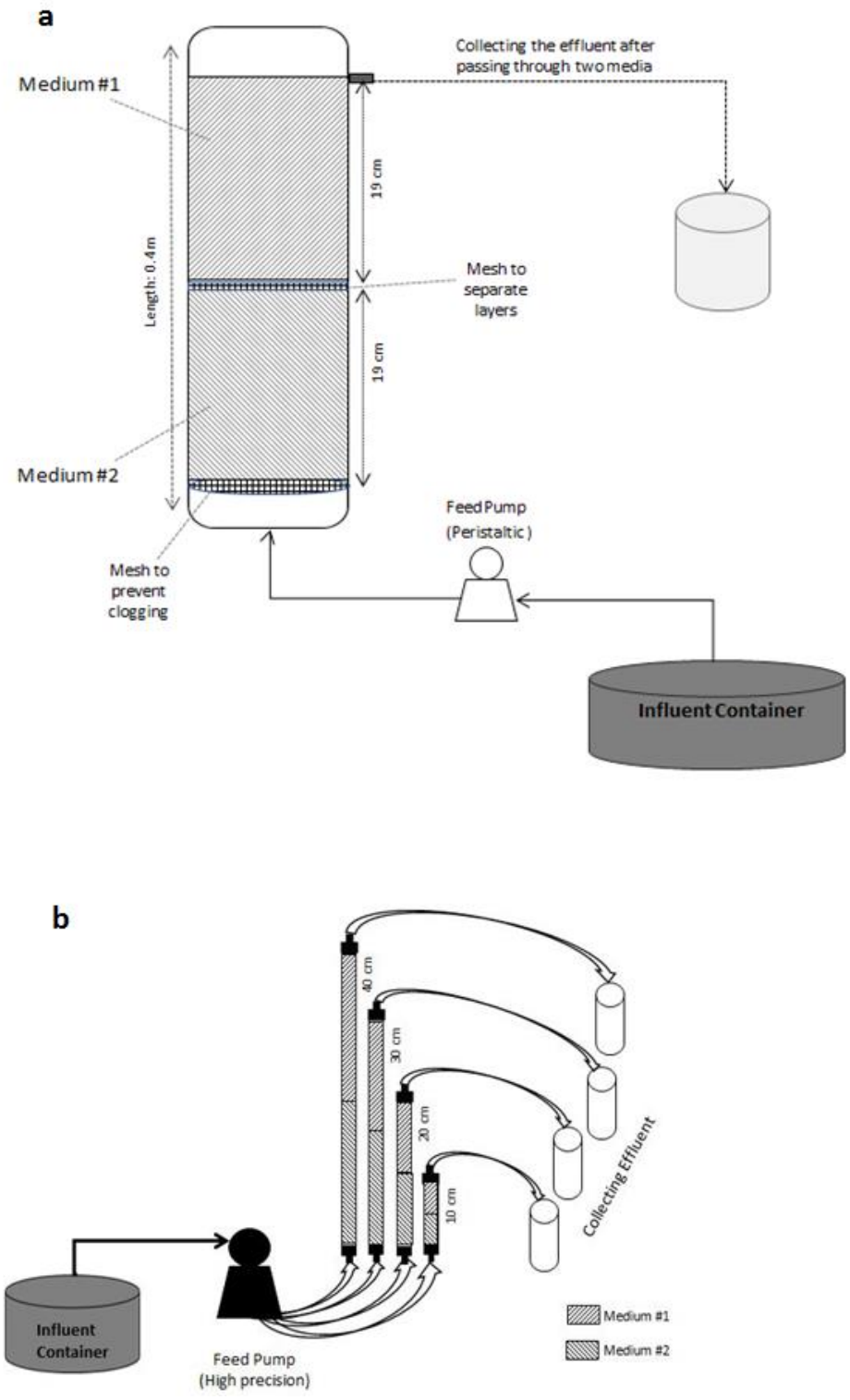

680

681

682

683 **Figure 2**

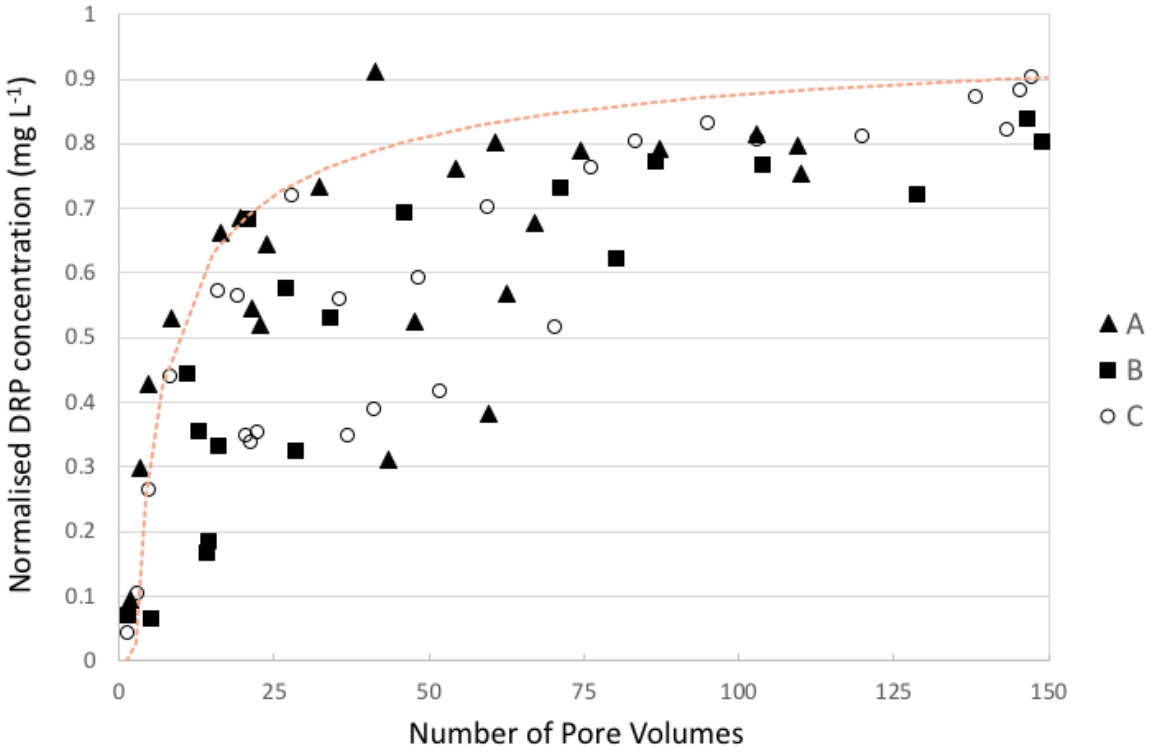

684

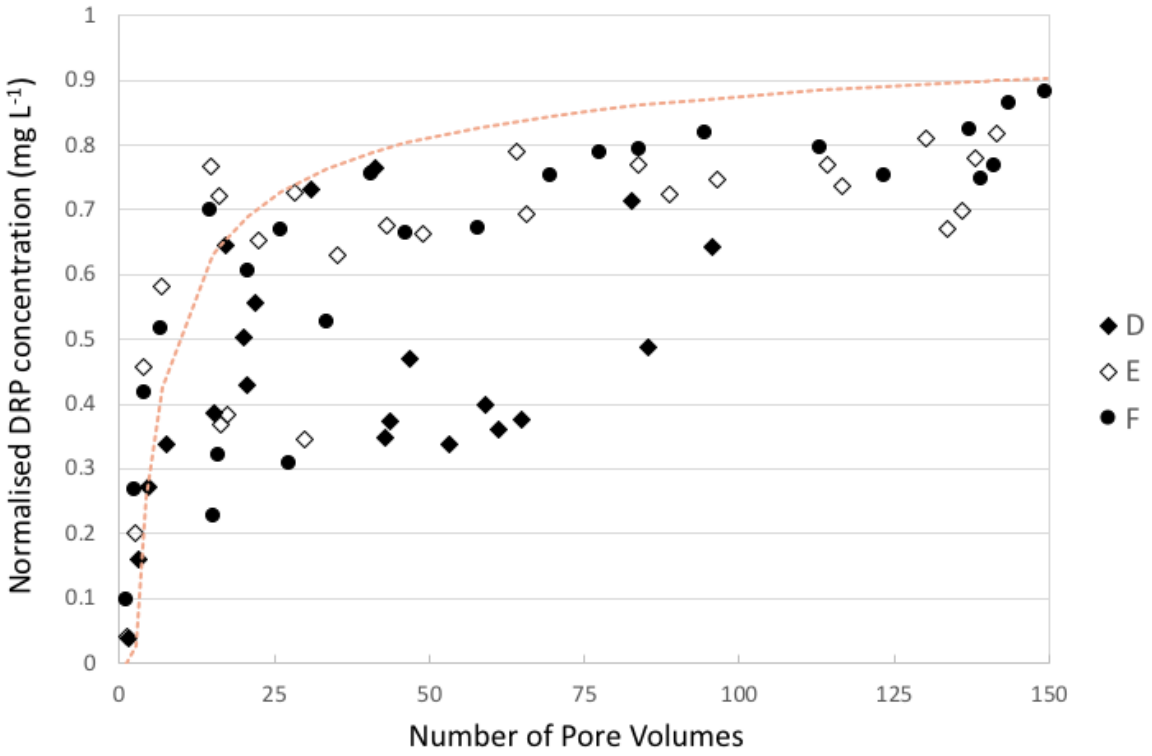

685

686

687 **Figure 3**

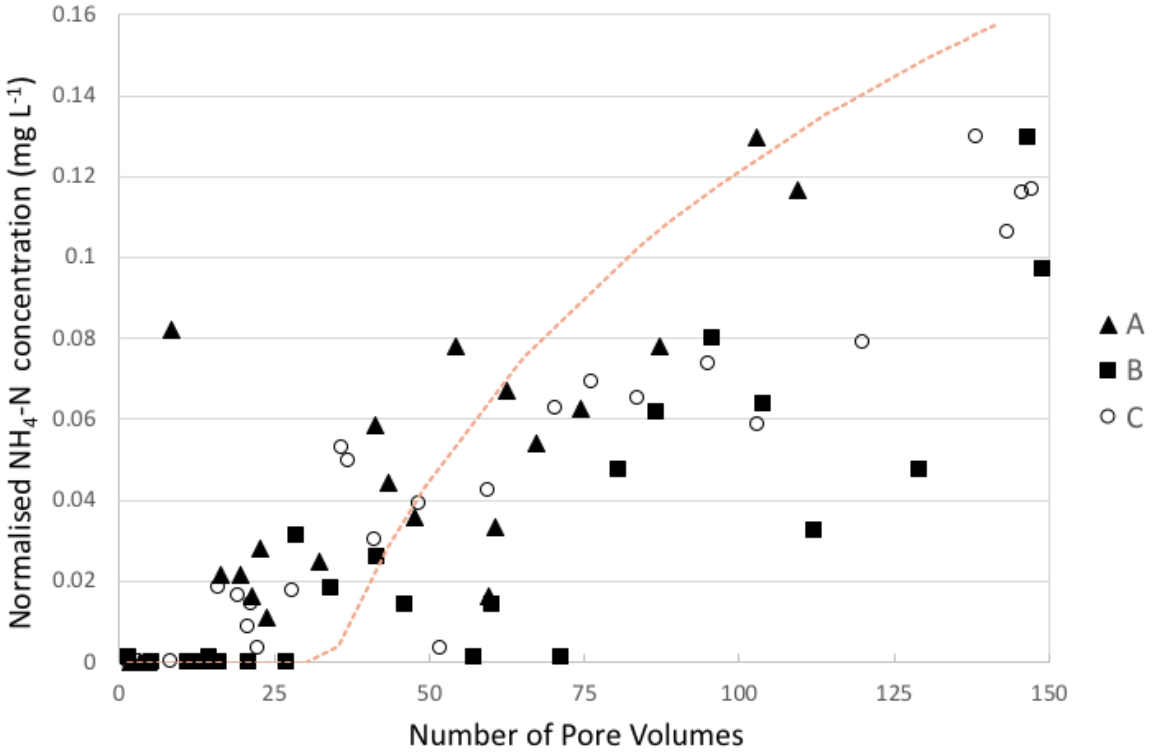

688

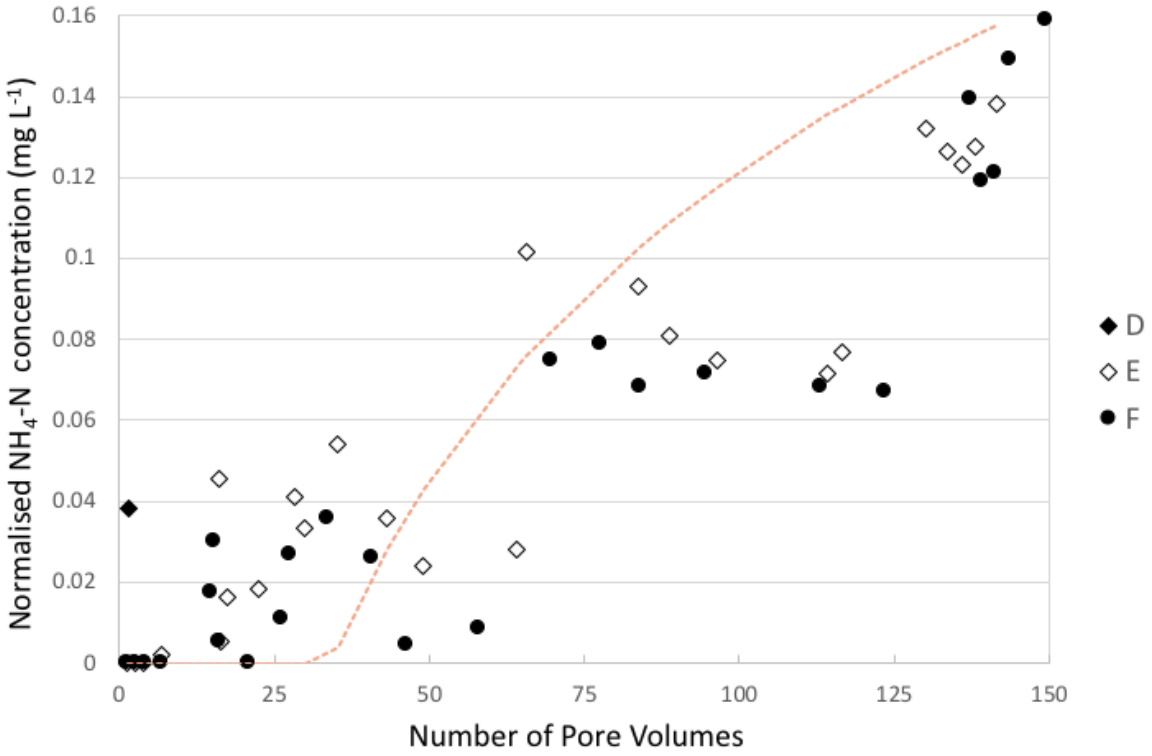

689

690

691 **Figure 4**

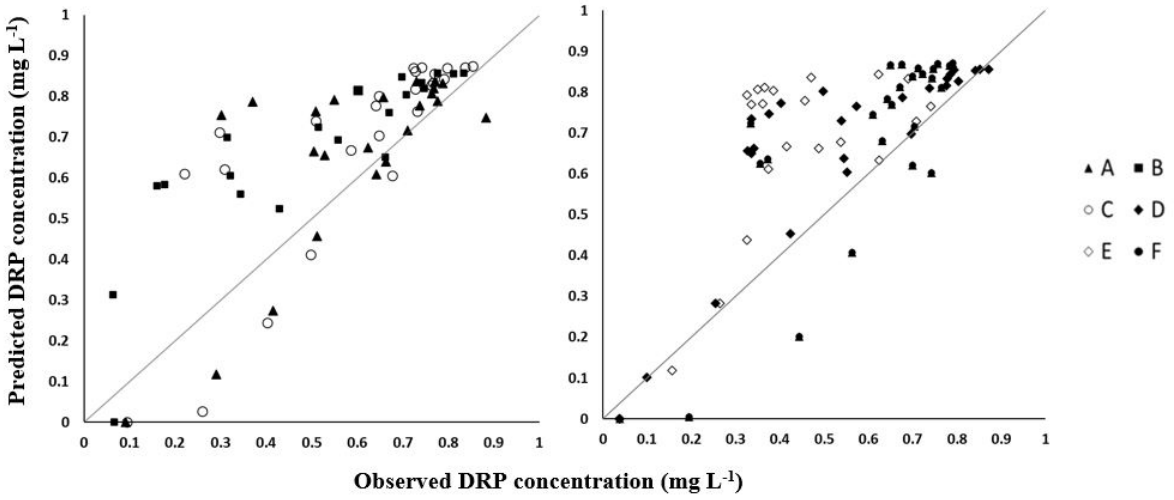

692

693

694

695

696

697

698

699

700

701

702

703

704

Figure 5

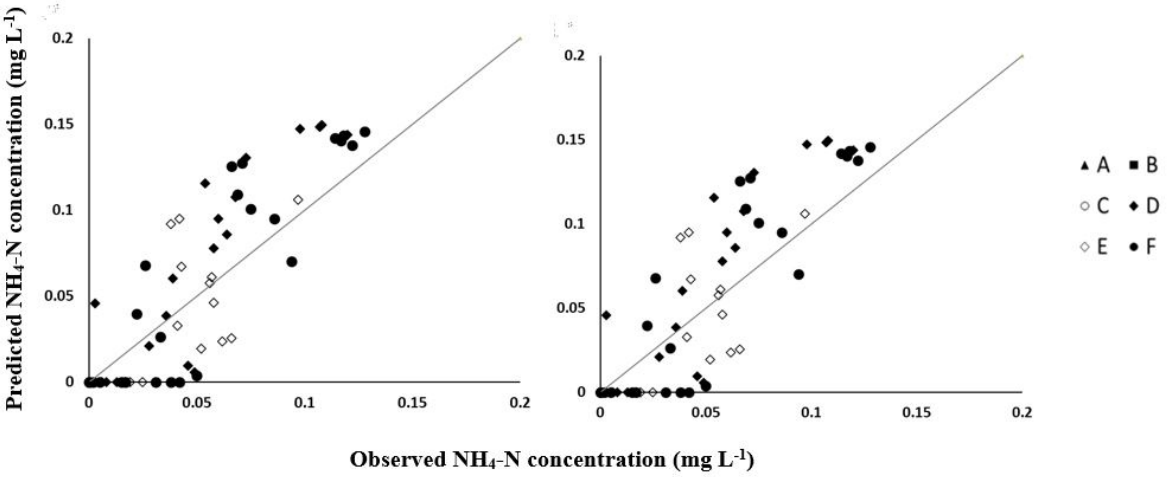
Predicted NH4-N concentration (mg L-1)
0.2
0.15
0.1
0.05
0
0
0.05
0.1
0.15
0.2
A
B
C
D
E
F
Observed NH4-N concentration (mg L-1)

719 **Figure 6**

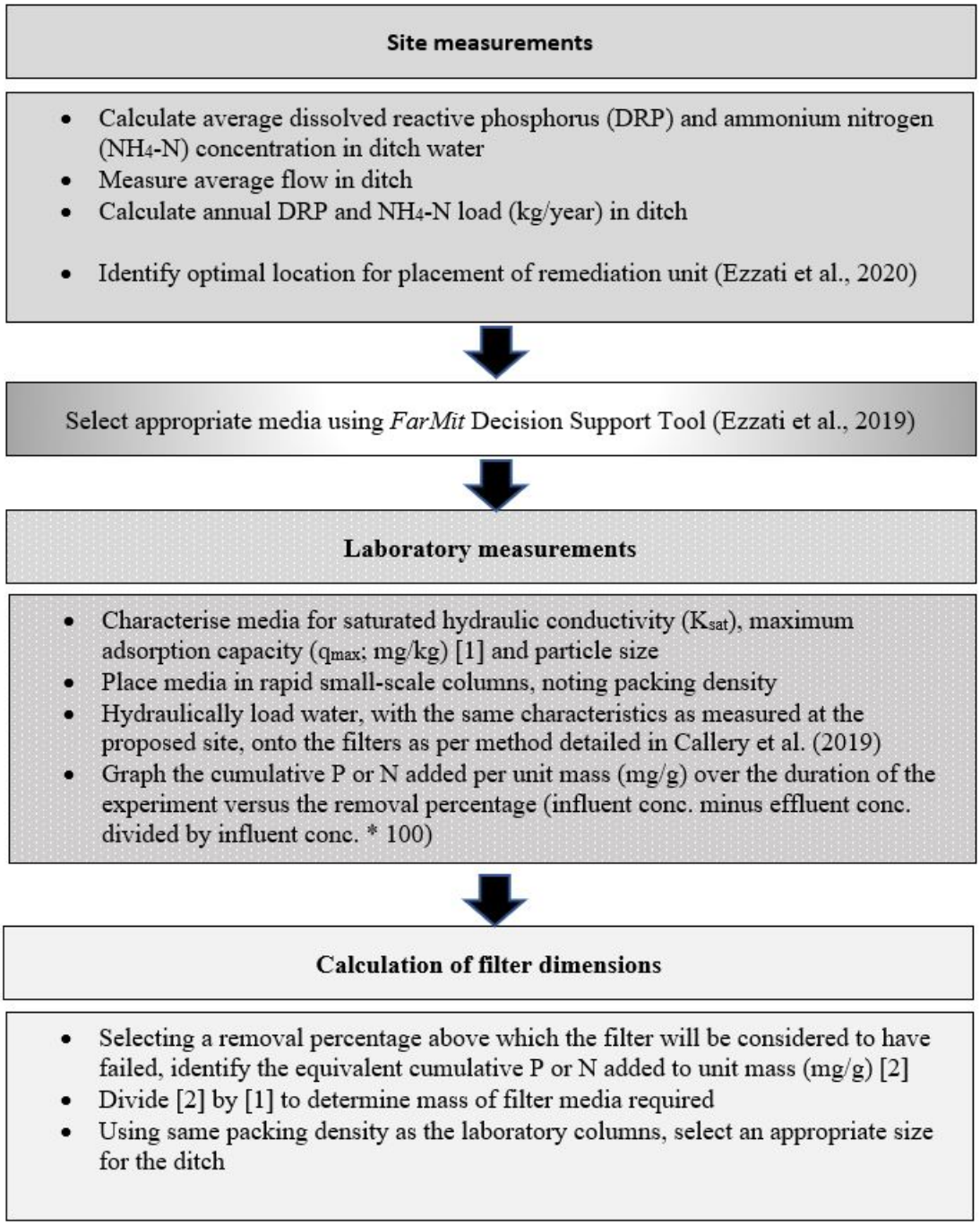

720